Journal of Sound and Vibration (1999) **227**(1), 230–238
Article No. jsvi.1999.2357, available online at http://www.idealibrary.com on IDEAL®

EXPERIMENTAL STUDY OF CHAOS IN A DRIVEN TRIPLE PENDULUM

Q. ZHU AND M. ISHITOBI

Department of Mechanical Engineering and Materials Science, Faculty of Engineering, Kumamoto University, 2-39-1 *Kurokami*, *Kumamoto* 860-8555, *Japan*

(*Received* 24 *August* 1998, *and in final form* 17 *May* 1999)

1. INTRODUCTION

Interest in periodically forced pendulums which can display chaotic motions has been quite widespread. Many researchers have been actively investigating the complex responses of the system experimentally. Beckert *et al.* [1] studied a forced non-linear torsion pendulum by measuring a bifurcation diagram which showed period doubling and chaos. Blackburn *et al.* [2] reported experimental observations of chaos in a driven, damped pendulum in which steady and alternating torques were applied. Driven pendulums with chaotic motions were also found by Heng *et al.* [3], Korte *et al.* [4], and others [5, 6]. Although the experiments mentioned above yield important information about the complex dynamics of periodically driven pendulums, the pendulums in these studies were limited to only one degree of freedom. Due to the lack of a predictive rule for the chaotic responses of the periodically driven pendulum, the conditions of the chaotic motion in the pendulum with higher degrees of freedom are still unclear. For this reason, a harmonically forced triple pendulum with three degrees of freedom was constructed. The purpose was to study the driven pendulum experimentally, since it is a typical non-linear physical system that may exhibit a wide range of interesting dynamic motions. Meanwhile, it was also hoped to provide experimental evidence for the existence of chaos in such a system.

2. CHAOTIC VIBRATION OF THE PENDULUM

Figure 1 shows the driven triple pendulum system used in this study. The pendulum consists of three rigid poles with lengths of L_1, L_2, and L_3. Masses m_1 and m_2 are attached to joint B and joint C, respectively, whereas mass m_3 is attached to the end of the lowest pole. The pendulum can only move within the x–y plane. The displacement of joint A is restricted to the horizontal direction with the forced harmonic motion $x_a = A \sin \omega t$. With the masses of the three rigid poles being ignored. If α, β, and γ are defined as the angular displacements of the three poles measured counter-clockwise from a vertical reference line, respectively, then

0022-460X/99/410230 + 09 $30.00/0

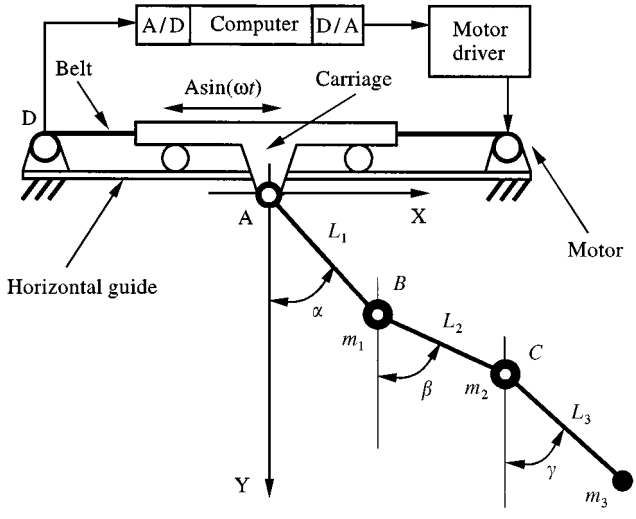

Figure 1. Schematic diagram of the horizontal forced triple pendulum and experimental apparatus. A/D and D/A: Contec AD16-16(PC)EH. Motor Driver: Japan E.M, IPS-1002C. A: Potentiometer, Midori Precisions, CPP-35B, B, C: Potentiometer, Copal Electronics, JC30S. D: Potentiometer, Midori Precisions CPP-35B.

the Euler–Lagrange equations of motion give

$$ML_1^2\ddot{\alpha} + m_{23}L_1L_2\ddot{\beta}\cos(\alpha-\beta) + m_3L_1L_3\ddot{\gamma}\cos(\alpha-\gamma) + m_{23}L_1L_2\dot{\beta}^2\sin(\alpha-\beta) + m_3L_1L_3\dot{\gamma}^2\sin(\alpha-\gamma) + c_1\dot{\alpha} + MgL_1\sin\alpha + ML_1\ddot{x}_a\cos\alpha = 0, \tag{1}$$

$$m_{23}L_1L_2\ddot{\alpha}\cos(\alpha-\beta) + m_{23}L_2^2\ddot{\beta} + m_3L_2L_3\ddot{\gamma}\cos(\beta-\gamma) - m_{23}L_1L_2\dot{\alpha}^2\sin(\alpha-\beta) + m_3L_2L_3\dot{\gamma}^2\sin(\beta-\gamma) + c_2(\dot{\beta}-\dot{\alpha}) + m_{23}gL_2\sin\beta + m_{23}L_2\ddot{x}_a\cos\beta = 0, \tag{2}$$

$$m_3L_1L_3\ddot{\alpha}\cos(\alpha-\gamma) + m_3L_2L_3\ddot{\beta}\cos(\beta-\gamma) + m_3L_3^2\ddot{\gamma} - m_3L_1L_3\dot{\alpha}^2\sin(\alpha-\gamma) - m_3L_2L_3\dot{\beta}^2\sin(\beta-\gamma) + c_3(\dot{\gamma}-\dot{\beta}) + m_3gL_3\sin\gamma + m_3L_3\ddot{x}_a\cos\gamma = 0, \tag{3}$$

where

$$\alpha = \alpha(t), \qquad \beta = \beta(t), \qquad \gamma = \gamma(t)$$

and

$$M = \sum_{i=1}^{3} m_i, \qquad m_{23} = \sum_{i=2}^{3} m_i, \qquad \ddot{x}_a = -A\omega^2\sin\omega t, \qquad \omega = 2\pi f.$$

The parameters c_1, c_2, and c_3 are damping coefficients of joints A, B, and C, respectively, and f is the forcing frequency in Hertz. The dot stands for time derivation. Equations (1)–(3) are non-linear and can only be integrated numerically.

As shown in Figure 1, the upper end of the pendulum is fixed to the rotator of a potentiometer, which is attached to the carriage. The potentiometer thus forms the joint A and the angular displacement α can be obtained directly by measuring the output voltage of the potentiometer. The carriage is driven by a DC motor via a belt and can move along a horizontal guide, which applies a forced motion to the upper end of the pendulum. The displacement of the carriage is measured by a potentiometer which is connected to the shaft of the support wheel of the belt. To ensure that the motion of the carriage is exactly $x_a = A \sin \omega t$, a personal computer with Intel 300 MHz Pentium II Processor is used, which is equipped with an A/D and D/A converter to give a 16-bit accuracy for input and output. The motion of the carriage is controlled by the computer with PID feedback control technique. Specifically, the amplitude is controlled by means of a motor driver, while the frequency is controlled by using RDTSC instruction of the CPU. By employing this controlling method, the carriage can have satisfactory harmonic movement with the maximum amplitude of 0·360 m. Two more potentiometers, one connecting the pole L_1 and the pole L_2, the other connecting the pole L_2 and the pole L_3, form the joints B and C respectively. The angular displacements α, β and γ can thus be obtained with the output voltages of the potentiometers in joints A, B, and C. In this design, the independent linearity of each of the potentiometers is $\pm 0{\cdot}5\%$. Since the diameter of the conducting wires for power supply to each potentiometer and for the voltage output from it is only 0·002 m, the effect of the conducting wires on the pendulum system can be ignored.

Experiments were carried out with various combinations of poles and masses. One of the sets of parameters for observing chaotic motion are $L_1 = L_2 = 0{\cdot}150$ m, $L_3 = 0{\cdot}200$ m, $m_1 = m_2 = m_3 = 0{\cdot}050$ kg. The three poles of the pendulum are made of aluminium alloy. The diameter of each pole is 0·003 m. The poles L_1 and L_2 weigh 0·003 kg each, while the pole L_3 weighs 0·004 kg. The masses m_1 and m_2 are the sum of the masses of the potentiometers, connectors that fix the potentiometers to the poles, and an additional mass for adjusting the total mass. The amplitude of the forcing displacement of the carriage was kept at $A = 0{\cdot}062$ m, a typical value in our experiments. The detection for chaotic response of the pendulum was started with an initial forcing frequency of $f = 0{\cdot}01$ Hz, and was repeated by increasing the forcing frequency with an increment of 0·01 Hz. Each new detection was started after the pendulum returned to the static state. It was observed that, if the forcing frequency was relatively low, the responses of the pendulum were periodic, with the three poles of the pendulum oscillating back and forth symmetrically to the vertical reference line. As the forcing frequency was increased to 1·667 Hz, the motion of the three poles of the pendulum became random-like simultaneously and the displacements α, β and γ were within $\pm \pi$. The time histories, phase-plane trajectories and power spectra related to α, β, and γ are shown in Figures 2–4. The phase-plane trajectories in Figures 2(b), 3(b), and 4(b) were plotted with the data sampled in 30 s and the power spectra in Figures 2(c), 3(c) and 4(c) were calculated from the data sampled in 6 min with a sampling

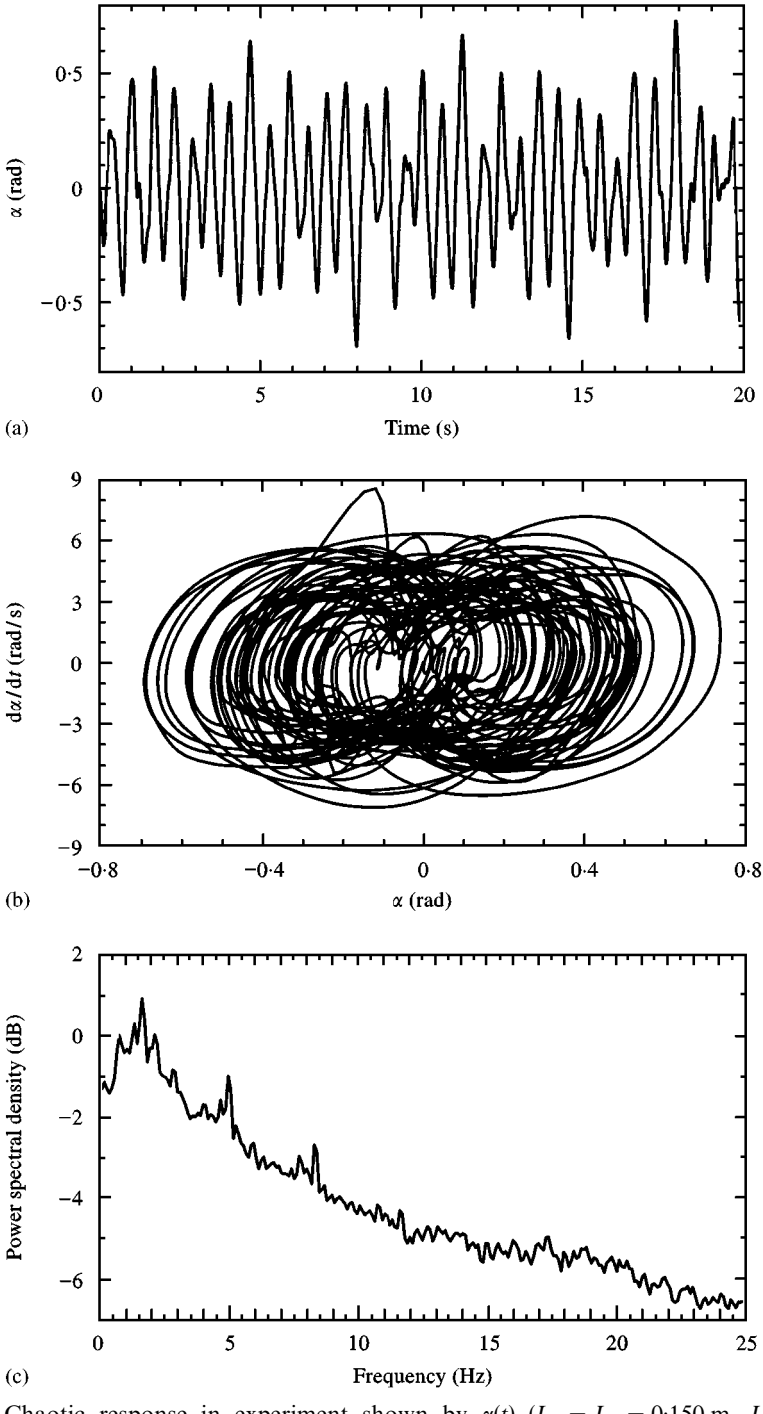

Figure 2. Chaotic response in experiment shown by $\alpha(t)$ ($L_1 = L_2 = 0{\cdot}150$ m, $L_3 = 0{\cdot}200$ m, $m_1 = m_2 = m_3 = 0{\cdot}050$ kg, $A = 0{\cdot}062$ m, and $f = 1{\cdot}667$ Hz): (a) time history of $\alpha(t)$, (b) phase-plane motion, (c) power spectrum of the time series of $\alpha(t)$.

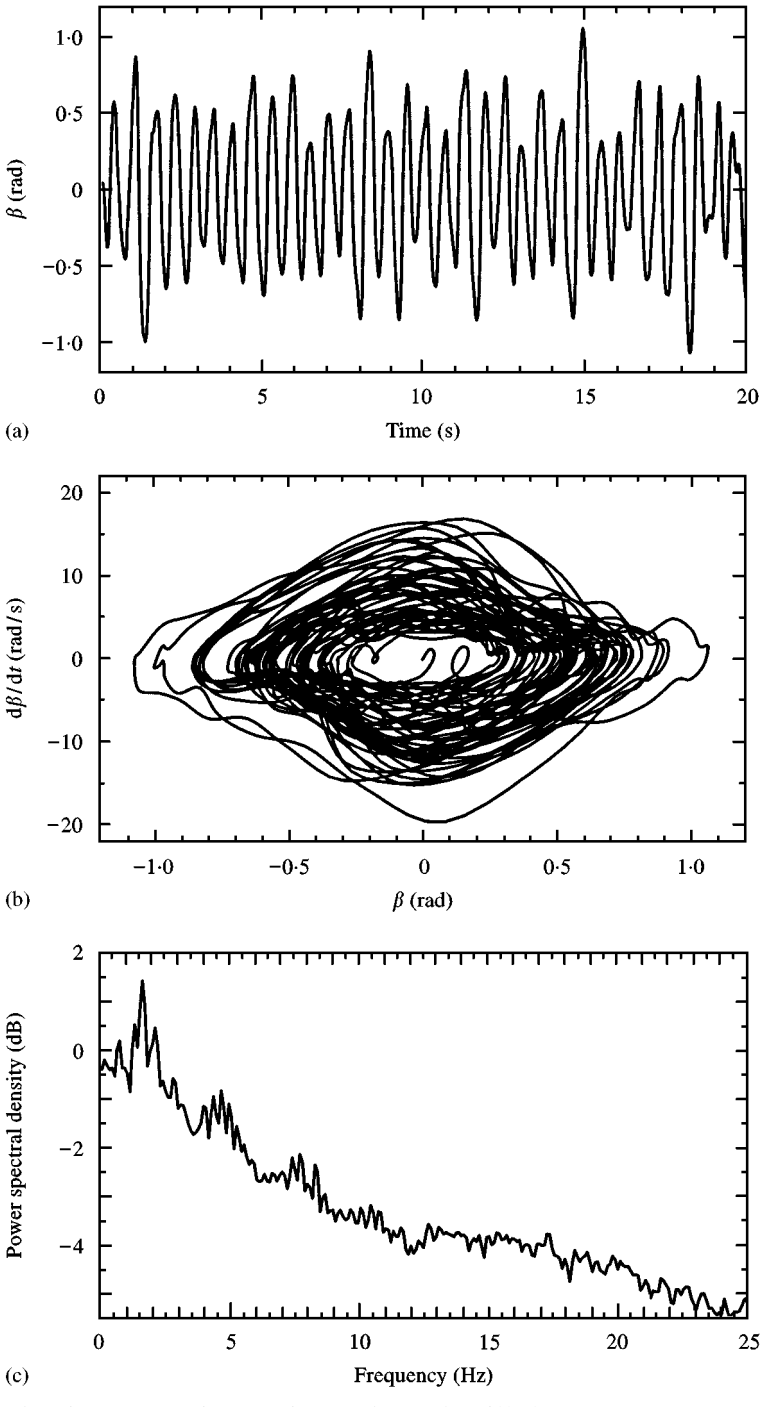

Figure 3. Chaotic response in experiment shown by $\beta(t)$ ($L_1 = L_2 = 0{\cdot}150$ m, $L_3 = 0{\cdot}200$ m, $m_1 = m_2 = m_3 = 0{\cdot}050$ kg, $A = 0{\cdot}062$ m, and $f = 1{\cdot}667$ Hz): (a) time history of $\beta(t)$, (b) phase-plane motion, (c) power spectrum of the time series of $\beta(t)$.

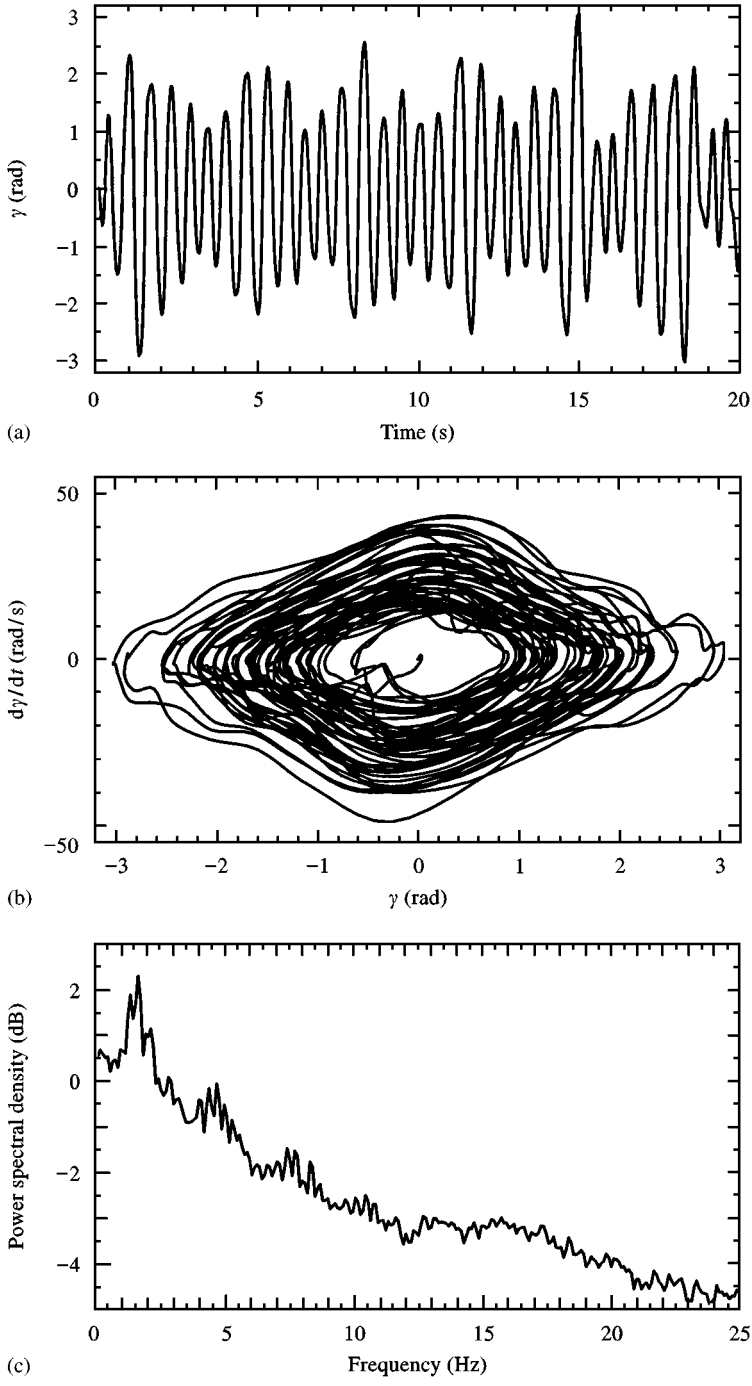

Figure 4. Chaotic response in experiment shown by $\gamma(t)$ ($L_1 = L_2 = 0{\cdot}150$ m, $L_3 = 0{\cdot}200$ m, $m_1 = m_2 = m_3 = 0{\cdot}050$ kg, $A = 0{\cdot}062$ m, and $f = 1{\cdot}667$ Hz): (a) time history of $\gamma(t)$, (b) phase-plane motion, (c) power spectrum of the time series of $\gamma(t)$.

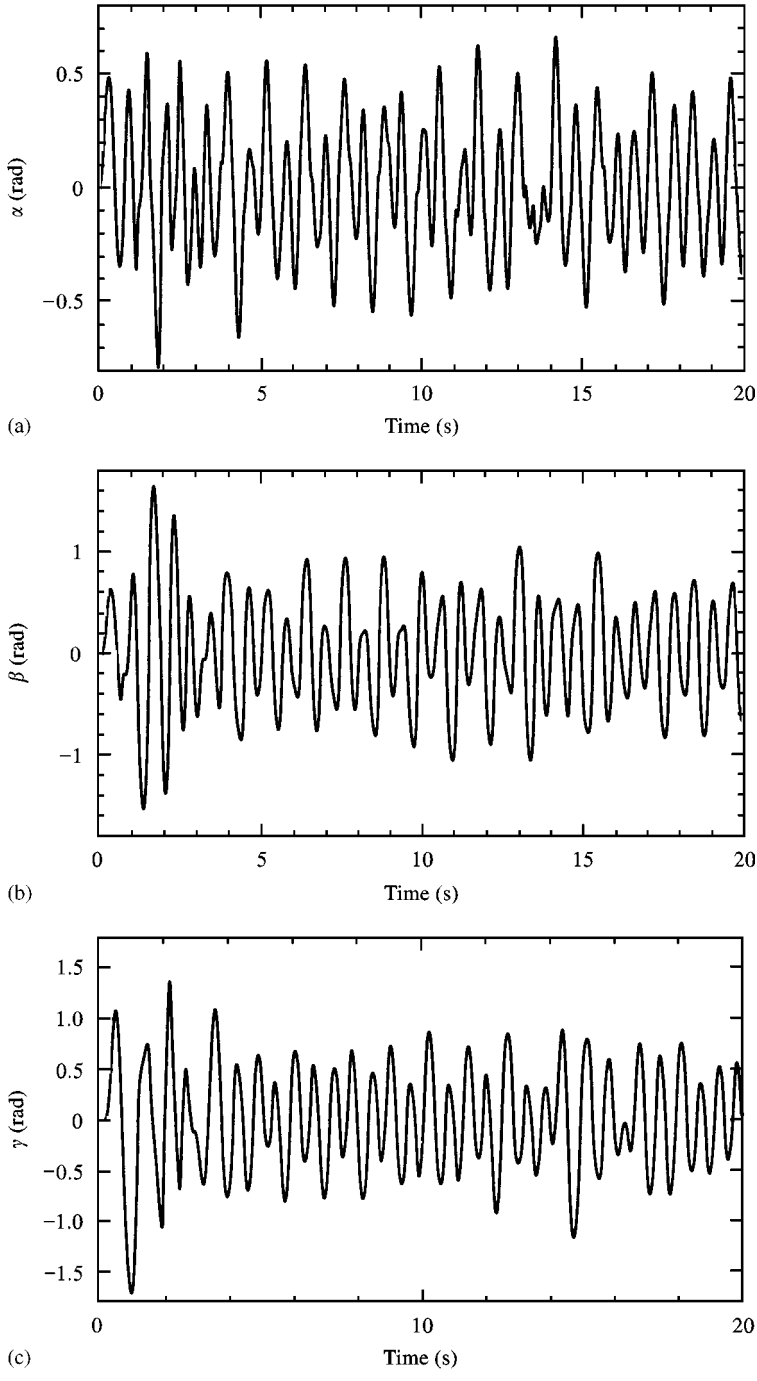

Figure 5. Time histories of chaotic responses of the pendulum in numerical simulation with parameters $L_1 = L_2 = 0{\cdot}150$ m, $L_3 = 0{\cdot}200$ m, $m_1 = m_2 = m_3 = 0{\cdot}050$ kg, $A = 0{\cdot}062$ m, and $f = 1{\cdot}667$ Hz, $c_1 = 1{\cdot}1996 \times 10^{-3}$ N m s/rad, and $c_2 = c_3 = 5{\cdot}9963 \times 10^{-4}$ N m s/rad. (a) time history of $\alpha(t)$, (b) time history of $\beta(t)$, (c) time history of $\gamma(t)$.

frequency of 50 Hz. Because there was no single criterion that could be used to determine whether the time history from the experiment was chaotic [7], the correlation dimension D_2 and the dominant Lyapunov exponent of the measured time history were investigated. Since the frequencies of the pendulum responses were relatively low, the noise in the measured signals could be ignored. The Grassberger–Procaccia algorithm [8, 9] was used to estimate D_2 and Wolf's algorithm [10] was used to calculate the dominant Lyapunov exponent. The displacements of α, β, and γ were sampled with a sampling period of 0·02 s and each data was 18 000 samples long. To create time-embedded vectors in the computation, the time delay value was determined by the use of average mutual information [11]. The computation gave the values of D_2 for $D_{2\alpha} = 2{\cdot}85$, $D_{2\beta} = 2{\cdot}68$, and $D_{2\gamma} = 2{\cdot}77$. On the other hand, the dominant Lyapunov exponents calculated were $\lambda_\alpha = 3{\cdot}85$, $\lambda_\beta = 3{\cdot}64$ and $\lambda_\gamma = 3{\cdot}49$ in the unit of bits/s. These results indicated that the motions of the three links of the triple pendulum shown in Figures 2(a), 3(a), and 4(a) were chaotic.

The numerical simulation was also carried out to confirm the existence of chaos in the system. Before the computation, the damping coefficients of c_1, c_2, and c_3 should be known. However, accurate determination of the actual damping characteristics to be used in the numerical simulations is very difficult, because of the difficulty in describing a physical system with a mathematical model. Because the main source for damping in the triple pendulum was dissipation in the bearings of the potentiometers, it was determined that linear viscous damping could be used to approximate the actual one. To measure the damping coefficients of the potentiometers, each of the potentiometers was used to construct a one-degree-of-freedom pendulum with a pole and a mass. The damping coefficient of each potentiometers was then measured and the values of $c_1 = 1{\cdot}1996 \times 10^{-3}$ N m s/rad and $c_2 = c_3 = 5{\cdot}9963 \times 10^{-4}$ N m s/rad were obtained approximately. The experimental parameters ($L_1 = L_2 = 0{\cdot}150$ m, $L_3 = 0{\cdot}200$ m, $m_1 = m_2 = m_3 = 0{\cdot}050$ kg, $A = 0{\cdot}062$ m, and $f = 1{\cdot}667$ Hz) were taken into equations (1), (2), and (3) for the numerical simulation. The motion equations of the pendulum were integrated using a variable time step, fourth order Runge–Kutta routine [12], with relative error of 10^{-8}, absolute error of 10^{-10} and time interval of $1{\cdot}5 \times 10^{-3}$ s. Because numerical integration can give spurious results with regard to the existence of chaos due to insufficiently small time steps [13], the step size was verified to ensure no such results were generated as a result of time discretization. The results of numerical simulation are shown in Figure 5. Although the time histories of α, β and γ in this plot are not the same as the ones in Figures 2(a), 3(a), and 4(a), they nonetheless suggest chaotic responses.

3. CONCLUSIONS

The experiments reported here show that a harmonically driven triple pendulum can exhibit chaotic motions even when the forcing inputs are highly deterministic. To our knowledge, this is the first time that chaotic motion has been observed experimentally in this particular type of driven pendulum.

REFERENCES

1. S. Beckert, U. Schock, C. D. Schulz, T. Weidlich and F. Kaiser 1985 *Physics Letters* **107A**, 347–350. Experiments on the bifurcation behaviour of a forced nonlinear pendulum.
2. J. A. Blackburn, Z. J. Yang and S. Vik 1987 *Physica* **26D**, 385–395. Experimental study of chaos in a driven pendulum.
3. H. Heng, R. Doerner, B. Hübinger and W. Martienssen 1994 *International Journal of Bifurcation and Chaos* **4**, 751–760. Approaching nonlinear dynamics by studying the motion of a pendulum. I. Observing trajectories in state space.
4. R. J. De Korte, J. C. Schouten and C. M. Van Den Bleek 1995 *Physical Review* **E 52**, 3358–3365. Experimental control of a chaotic pendulum with unknown dynamics using delay coordinates.
5. J. Starett and R. Tagg 1995 *Physical Review Letters* **74**, 1974–1977. Control of a chaotic parametrically driven pendulum.
6. D. J. Christini, J. J. Collins and P. S. Linsay 1996 *Physical Review* **E 54**, 4824–4827. Experimental control of high-dimensional chaos: the driven double pendulum.
7. S. Haykin and S. Puthusserypady 1997 *Chaos* **7**, 777–802. Chaotic dynamics of sea clutter.
8. P. Grassberger and I. Procaccia 1983 *Physical Review Letters* **50**, 346–349. Characterization of strange attractors.
9. H. Takayasu (editor) 1987 *Fractal Science*. Tokyo: Asakura Shouten (in Japanese).
10. A. Wolf, J. B. Swift, H. L. Swinney and J. A. Vastano 1985 *Physica* **16D**, 285–317. Determining Lyapunov exponents from a time series.
11. A. M. Fraser and H. L. Swinney 1986 *Physical Review* **A 33**, 1134–1140. Independent coordinates for strange attractors from mutual information.
12. C. Watabe, R. Natori and R. Okuni (editors) 1989 *Software for Numerical Calculation with Fortran 77*. Toyko: Maruzen Inc. (in Japanese).
13. B. H. Tongue 1987 *American Society of Mechanical Engineers, Journal of Applied Mechanics* **54,** 695–699. Characteristics of numerical simulations of chaotic system.